Comparative study of Cu_2XSnS_4 (X = Ni, Co, Mn or Fe) films synthesized by spray pyrolysis under air atmosphere, as suitable absorber layers for photovoltaic applications.

S. Dridi[1,2*], N. Bitri[1], E. Aubry[3,4], P. Briois[3]

[1]Université de Tunis El Manar, Ecole Nationale d'Ingénieurs de Tunis, Laboratoire de Photovoltaïque et matériaux semi-conducteurs, 1002, Tunis, Tunisie.

[2]Université de Tunis, Ecole Nationale Supérieure d'Ingénieurs de Tunis.

[3]Institut FEMTO-ST, UMR 6174, CNRS, Université de Bourgogne Franche-Comté, UTBM, rue Ernest Thierry-Mieg, Site de Montbéliard, 90010 Belfort cedex, France

[4]Institut FEMTO-ST, UMR 6174, CNRS, Université de Bourgogne Franche-Comté, UFC, 2 place Lucien Tharradin, Site de Montbéliard, 25200 Montbéliard, France

[*]E-mail: dridisarra13@gmail.com

Abstract

The present work deals with the synthesis of an absorber Cu_2XSnS_4 sulfide (X = Ni, Fe, Co or Mn) thin films by a spray pyrolysis method on hot substrate and under air atmosphere for low cost solar cell. Chemical composition analyzes by energy-dispersive X-ray spectroscopy (EDS) revealed the presence of all the chemical elements (Cu, Sn, S and Co, Ni, Mn or Fe) with a composition close to the stoichiometry of the layers of Cu_2NiSnS_4 (CNTS), Cu_2CoSnS_4 (CCTS) and far from the stoichiometry for the layers of Cu_2MnSnS_4 (CMTS) and Cu_2FeSnS_4 (CFTS). The X-ray diffraction (XRD) analyzes showed the crystallization of the desired phase such as the cubic phase of CNTS with a preferential orientation (111) and the stannite phase of CCTS and CMTS with a preferential orientation (112), except for the CFTS film which is poorly crystallized. SEM analyzes show that CNTS, CCTS and CMTS layers exhibit a rather homogeneous and compact surface with nodule distribution. The CFTS layer surface shows excrescences separated by voids leading to a porous and diffusing surface. The optical analyzes indicated a high absorption coefficient of the order of 10^4 cm^{-1} in the visible range for all the layers and an optical band gap of 1.62, 1.58 and 1.64 eV for the layers CNTS, CCTS and CMTS respectively, whereas the direct band gap of CFTS film is higher (~ 2.23 eV). The comparison of CXTS films synthesized in the same conditions demonstrates that the CNTS and CCTS films have the most suitable features (optical, electrical, mechanical and oxidation resistance) to be use as absorbing layer in low cost solar cell.

Keywords: Thin films, chemical synthesis, photovoltaic, semiconductors, chalcogenides, spray pyrolysis.

Introduction

The significant development of the market for new technologies, the multiplication of their functionalities and their miniaturization explain the growing interest in renewable energy resources, including solar energy. The latter is a promising energy option on a human scale considered as an inexhaustible natural resource unlike fossil resources which are polluting and dangerous for the planet as well. In addition, solar energy would be widely used in different sectors such as: industry, agriculture and daily life in general. To cope with a growth in global electricity consumption, photovoltaic systems will have to be put in place to meet the needs of the growing consumption.

The main generations of photovoltaic cells studied so far are the generation of silicon, the generation of thin-film solar cells, that of organic cells, multi-junction cells, even nowadays dye cells and many others…As part of this work, our focus has been on thin-film solar cell technology. In this technology, solar cells based on Cu_2XSnS_4 quaternary semiconductor (X = Mn, Fe, Co, Ni, Zn, etc.) as absorbing materials are particularly interesting. These materials are also well suited for utilization in low cost solar cells, due to their similar crystal structure with $Cu(In,Ga)(S,Se)_2$ (CIGS), $CuInSe_2$ (CIS) and CdTe, their suitable band gap and high absorption coefficient. However, the scarcity of Indium and Gallium and the toxicity of Cadmium acts as an obstacle for large-scale production of CIGS, CIS and CdTe thin film solar cell.

Recent studies show that Cu_2ZnSnS_4 (CZTS) has potentially excellent properties. Its application in photovoltaic device has been allowed by abundant, inexpensive and non-toxic elements. The physical properties would make CZTS to be the best absorber compared to other chalcogenides. This semi-conductor has a p-type behavior, an optimum optical band gap of 1.55 eV and a high absorption coefficient ($\sim 10^4$ cm^{-1}) [1,2]. Therefore, it is important to develop and explore related compounds of CZTS such as, Cu_2NiSnS_4 (CNTS), Cu_2FeSnS_4 (CFTS), Cu_2CoSnS_4 (CCTS) and Cu_2MnSnS_4 (CMTS).

Besides, the spray pyrolysis technique is one of the low-cost thin film deposition methods and has the advantage of being simple and economical. Indeed, the feasibility to synthesize CMTS absorbing layer by spray pyrolysis under air atmosphere without any expensive oxidation

precaution was demonstrated [3]. To avoid the formation of undesired harmful oxides, the deposition temperature must be low, but sufficiently high to ensure a rather good crystallization of the sulfide for optimal properties. Another important advantage for the use of this method is the possibility of obtaining large surfaces of the material. The present work focuses on the use of the spray pyrolysis technique for the deposition of thin layers of CNTS and its counterparts such as CCTS, CFTS and CMTS, thus allowing a comparative study of the main physical features of the CXTS thin films independently of the method used.

Experimental section

Elaboration details

The idea here is to carry out a comparative study between the four different materials namely CNTS, CCTS, CFTS and CMTS. In this series of manipulations, the aqueous solutions used are formed from the following precursors ($CuCl_2.2H_2O$), ($NiCl_2.6H_2O$), ($CoCl_2.6H_2O$), ($FeCl_2.4H_2O$), ($MnCl_2.4H_2O$), ($SnCl_2.2H_2O$) and thiourea (CH_4N_2S) as sulfur source. In the present report, four different samples were prepared for comparison. A similar synthesis strategy was developed based on the previous reports [3]. In a typical synthesis, the starting solutions were prepared in four different glass bottles consisting of $(SC(NH_2))_2$ (32 mmol), XCl_2 (X = Mn, Fe, Co, Ni) (2 mmol), $SnCl_2$ (2 mmol) and $CuCl_2$ (4 mmol) by dissolving in distilled water as the solvent agent. Then, 0.5 mL of HCl was poured into the mixtures under continuously stirring to get homogeneous solutions. For every solution used, the thiourea was introduced in excess relative to the other elements to compensate for the loss of sulfur during the deposition. Compressed air was used as a carrier gas. Further to make CNTS, CCTS, CFTS and CMTS thin films, the CXTS solutions (100 mL) were sprayed onto heated glass substrates at 280 °C with a fixed deposition time of 30 min in air. The substrates consist in microscope glass. As absorbing layer for photovoltaic application purpose, the thickness of the layer has been adjusted at about 1.8 ± 0.2 µm.

The main deposition conditions are summarized in table1.

Table 1. *Optimized conditions of the spray method.*

Deposit parameters	*Deposit conditions*
Spray deposition rate	3 10^{-3} L min^{-1}
Gas flow rate	10 LPM
Distance nozzle-substrate	20 cm
Nozzle rotation speed	14 rpm

The formation of CNTS, CCTS, CFTS and CMTS phases from solutions can be schematized by the global reactions:

$$2\ CuCl_2 + \mathbf{NiCl_2} + SnCl_2 + 4\ CH_4N_2S + 12\ H_2O \rightarrow \mathbf{Cu_2NiSnS_4} + 8\ NH_4Cl\uparrow + 4\ CO_2\uparrow + 4\ H_2O\uparrow \quad \textbf{Eq.1}$$

$$2\ CuCl_2 + \mathbf{CoCl_2} + SnCl_2 + 4\ CH_4N_2S + 12\ H_2O \rightarrow \mathbf{Cu_2CoSnS_4} + 8\ NH_4Cl\uparrow + 4\ CO_2\uparrow + 4\ H_2O\uparrow \quad \textbf{Eq.2}$$

$$2\ CuCl_2 + \mathbf{FeCl_2} + SnCl_2 + 4\ CH_4N_2S + 10\ H_2O \rightarrow \mathbf{Cu_2FeSnS_4} + 8\ NH_4Cl\uparrow + 4\ CO_2\uparrow + 2\ H_2O\uparrow \quad \textbf{Eq.3}$$

$$2\ CuCl_2 + \mathbf{MnCl_2} + SnCl_2 + 4\ CH_4N_2S + 10\ H_2O \rightarrow \mathbf{Cu_2MnSnS_4} + 8\ NH_4Cl\uparrow + 4\ CO_2\uparrow + 2\ H_2O\uparrow \quad \textbf{Eq.4}$$

- **Measurement instrument details**

The CXTS thin films were characterized by various complementary experimental methods. The morphology of the coatings was characterized by means of a Field Emission Scanning Electron Microscope (FE-SEM JEOL JSM-7800F). The chemical composition of the film deposited on glass substrates was estimated by energy-dispersive X-ray spectroscopy (Quantax Bruker with XFLASH 6|30 detector) coupled with the FEG-SEM. The structural properties of spray deposited films were studied by X-ray diffraction (Philips X'Pert diffractometer) with Cu-Kα radiation (λ = 1.5418 Å) operated in the scanning angle 2θ from 20 to 70°. UV-Vis spectrophotometer (type Shimadzu UV 3100S) was applied to ascertain the transmittance and reflectance measurements for determining the optical parameters such as the absorption coefficient and the band gap energy. The electrical characterizations were achieved at room temperature using the four-probe method, which is composed by a certified Jandel cell (Multi height probe, Jandel Engineering Limited, Lindslade, UK) with well-known factor form attached to an HP 3458A multimeter (Agilent, Massy, France) in order to measure the electrical resistivity of the thin film material. The conductivity type was investigated with the hot-point

method. A hot-point probe method enables an easy determination of the nature of the main charge carrier (n or p-type). Generally, the hot point probe experiment consists of a soldering iron, a milliammeter and a pair of probes. For the configuration, the hot and cold probes were connected simultaneously to the positive and negative terminal of the milliammeter, and were attached to a semiconductor surface. Then, the measurements of n-type films give a positive voltage reading in the milliammeter, while p-type film results in a negative voltage reading.

Results and discussion

Compositional characteristics

The chemical composition of all the layers as well as the atomic ratios namely Cu/(X+Sn), X/Sn and S/(Cu+X+Sn) are gathered in Table.1. For a stoichiometric chemical composition in CXTS material, all the atomic ratios must tend to 1. The CNTS film exhibits a fine excess in Ni and Cu, whereas the sulfur content is stoichiometric. CCTS layer is slightly enriched with Co, Cu and sulfur (S/metals ratio >1), suggesting that the sulfur was sufficiently incorporated within the layers throughout spraying. This is advantageous to decrease the sulfur vacancies and subsequently improve the crystalline quality of the thin layers of CCTS. This result was observed by J. He et al. who synthesized the thin layers of Cu_2ZnSnS_4 by the sputtering method [4]. For the CMTS layers, it is clearly seen that the composition is slightly rich in tin (Mn/Sn ratio < 1) and has a chemical composition lacking in sulfur since the S/metals ratio < 1. These deviations from the stoichiometry would lead to the appearance of secondary phases of the tin sulfide type. Similar results were also reported by M. Patel et al. for thin layers of Cu_2ZnSnS_4 deposited by spray pyrolysis [5]. For the CFTS layers, a very sulfur-deficient chemical composition was revealed (S/metals ratio of 0.3). This relatively strong deviation from stoichiometry could inhibit the crystallization of the stannite CFTS phase and could generate the formation of either secondary phases or complex type defects. While the EDS is not suitable technique for an accurate measurement of the oxygen, its content is relatively high in CFTS and in less extent in CMTS film. The strong oxidation in CFTS film could be the reason of the stoichiometric deviation in sulfur. The non oxidation observed in CNTS and CCTS compared to CMTS and CFTS is also the result of the less favorable free energy of formation of the Co and Ni oxides compared to that of Fe or Mn oxides.

Table 2. *Chemical composition of CXTS thin films deposited at substrate temperature of 280 °C during 30 min under air.*

Samples	*Atomic ratios*			*Composition (at. %)*
	Cu/(X+Sn)	*X/Sn*	*S/metals*	*[O]*
Expected ratios	1.0	1.0	1.0	-
CNTS	1.1	1.2	1.0	4.1
CCTS	1.1	1.1	1.1	10.0
CMTS	1.0	0.8	0.8	35.9
CFTS	1.0	1.0	0.3	45.6

- **Structural characteristics**

In Figures 1.a, 1.b, 1.c and 1.d the XRD diffractograms of the thin layers based on different materials are shown. From Figure 1.a relative to the CNTS layer, the presence of the cristallographic planes (111), (220) and (311) located at angles 2θ equal to 28.84°, 47.82° and 56.36° are clearly noted. They correspond to the cubic phase CNTS of the space group F-43m (JCPDS N° 00-026-0552) [6]. Nevertheless, peaks relating to the presence of secondary phases of NiS_2 in addition to the characteristic lines of CNTS are observed. The XRD diffractogram of Figure 1.b (CCTS layer) shows the presence of peaks (112), (211), (204) and (312) located at 2θ = 28.40°, 37.92°, 47.62° and 56.72° characteristic of the stannite phase of CCTS with the space group I-42m (JCPDS No. 00-026-0513) [7]. Again, in addition to this phase, the presence of other small peaks related to the secondary phases mainly of CoS_2 and traces CuS_2 is noticed. The formation of binary sulfides is rather in agreement with the chemical composition estimation. Indeed, the sulfur and metallic elements excesses measured by EDS in CNTS and CCTS lead to the crystallization of binary sulfides. No oxides crystallize according to the rather low deposition temperature, low standard Gibb's energies of simple oxide formation and poor oxygen content. In CMTS film (Figure 1.c), the presence of peaks (112), (204) and (303) located at 2θ = 28.45°, 47.33° and 56.43° characterizes the stannite tetragonal phase of CMTS in I-42m space group (JCPDS N° 01-089-1952) [8]. Moreover, the CMTS phase is followed by a very weak peak which could be attributed to the MnS_2 or SnS_2 phases. Referring to Table.1, the appearance of the secondary phase of the tin disulphide is more plausible given the high tin content. Besides, it can be observed of a weak diffraction line at about 22° which could be ascribed to MnO_2 phase in agreement with the oxygen content evolution in this film. From

Figure 1.d, a XRD diffractogram with weak diffraction lines is observed and is related to the poor crystallization of the stannite CFTS phase. This could prove the predominance of the amorphous phases. Considering the chemical analysis results (Table.1), the CFTS layer should be sulfur-deficient with a metal-rich composition. The high sulfur deficiency combined with high oxygen content is probably the reason of such result. The sprayed films of CNTS, CCTS and CMTS phases are well crystallized while the phase of CFTS exhibits poor crystallization. Moreover, it was shown that the CNTS material is preferentially oriented along the [111] direction, unlike the CCTS and CMTS materials which are preferentially oriented along the [112] direction characteristic of the stannite structure. Furthermore, the CNTS and CCTS film exhibits secondary phases mainly based on sulfides, whereas traces of manganese oxide and tin sulfide formation are detected in CMTS. Based on the hypothesis that CFTS film is more oxidized than its counterparts, the deposition temperature is probably insufficient to crystallize oxides. Consequently, among the materials belonging to the CXTS family (X = Mn, Fe, Co and Ni), the CNTS material is distinguished by a more pronounced crystallinity than the other CCTS and CMTS materials which are characterized by a less intense main peak at same deposition time.

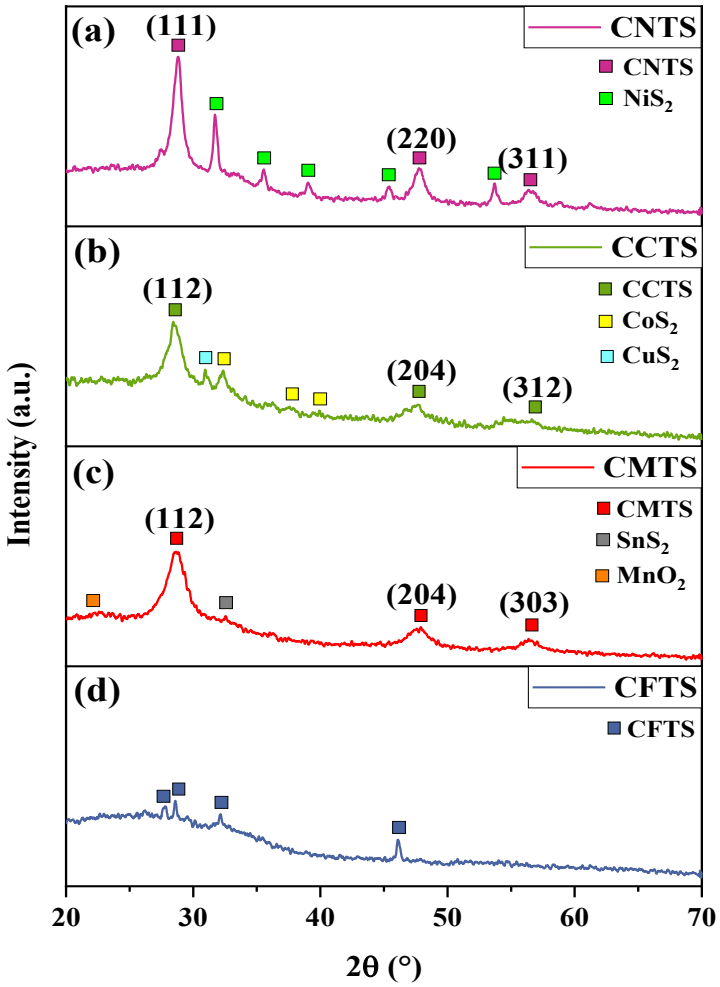

Figure 1. *X-ray diffractograms of* ***(a)****: CNTS,* ***(b)****: CCTS,* ***(c)****: CMTS and* ***(d)****: CFTS thin films deposited at substrate temperature of 280 °C during 30 min.*

From the XRD diffractograms (Figure.2), the size of the crystallites **(D)**, the microstrain **(ε)** and the dislocation density **(δ)** were calculated by referring to equations Eq.1, Eq.2 and Eq.3 [9,10,11]. The microstructural parameters of the various thin layers, namely CNTS, CCTS and CMTS, are calculated and collated in Table.2, except of CFTS which its crystallization is insufficient (k is the shape factor fixed arbitrary at 0.9 for spherical shape, β the Full Width at Half Maximum (FWHM) and θ the diffraction angle).

$$D = \frac{k\lambda}{\beta \cos(\theta)} \qquad \textbf{Eq.5}$$

$$\varepsilon = \frac{\beta}{4 \tan(\theta)} \qquad \textbf{Eq.6}$$

$$\delta = \frac{1}{D^2} \qquad \textbf{Eq.7}$$

Table 3. *Microstructural parameters of CNTS, CCTS and CMTS thin films deposited at substrate temperature of 280 °C during 30 min.*

Thin films	*2θ (°)*	*(hkl)*	*β (°)*	*D (nm)*	*ε (10^{-1})*	*δ (10^{-3} nm^{-2})*
CNTS	28.84	(111)	0.815	12	0.8	7.4
CCTS	28.40	(112)	1.126	7	1.1	18.8
CMTS	28.45	(112)	1.508	5	1.5	33.7

The calculation of the microstructural parameters was carried out from the main peaks of the XRD diffractograms. The average size of the crystallites calculated for the thin layers of CNTS, CCTS and CMTS is of the order of 12, 7 and 5 nm, respectively. These values are close to those reported by several researchers [3,12,13,14]. The evolution of the crystallite size combined with that of the X-ray intensity suggests that the CNTS layer develop a higher crystallinity than the CCTS or CMTS layers. Moreover, it can be noticed that the microstrains values are relatively low and increase contrary to the size of the crystallites while passing from the CNTS layer to the CMTS layer, meaning that the smaller crystallite size of CMTS should develop higher amount of defects or imperfections [15]. The lowest value of the dislocation density is obtained with the CNTS films, which confirms its higher crystallinity [14].

- **Topography characteristics**

Figures 2.a, 2.b, 2.c and 2.d illustrate the surface morphologies of thin layers of CNTS, CCTS, CMTS and CFTS. These secondary electron SEM micrographs show a difference in the surface state of the different layers. The micrograph corresponding to the CNTS surface (Figure 2.a) highlights a homogeneous and compact surface of the CNTS layers with an agglomerated distribution of very fine nodules (~ 100 nm) covering the entire surface of the substrate. The CCTS layer (Figure 2.b) presents also a compact surface with the presence of larger nodules of different sizes (~ 200-800 nm) distributed on the surface. The micrograph of the CMTS surface (Figure 2.c) reveals a compact surface with the presence of fine (~ 300 nm) and very large nodules (~few microns) dispersed on the surface. Such nodules would be related to the secondary phases formation (NiS_2 in CNTS, CoS_2 or CuS_2 in CCTS, SnS_2 or MnO_2 in CMTS). Cracking is also observed on the surface of the CMTS layers. This observation is explained by

the stress increase in the CMTS films. The surface of the CFTS layers present excrescences separated by voids leading to a porous layer (Figure 2.d). This topography would be the result of the relatively strong oxidation in CFTS and to the sulfur deficiency. These observations are in good agreement with the results of XRD and chemical contents. The thickness measured for the thin layers of CNTS, CCTS, CMTS and CFTS are respectively of the order of 1.6, 1.7, 1.9 and 2.0 μm, respectively. These last values are of the same order of magnitude as the suitable thicknesses of the absorbers [16,17]. However, the deposition time being constant, the progressive increase of the thickness would be related to the film oxidation.

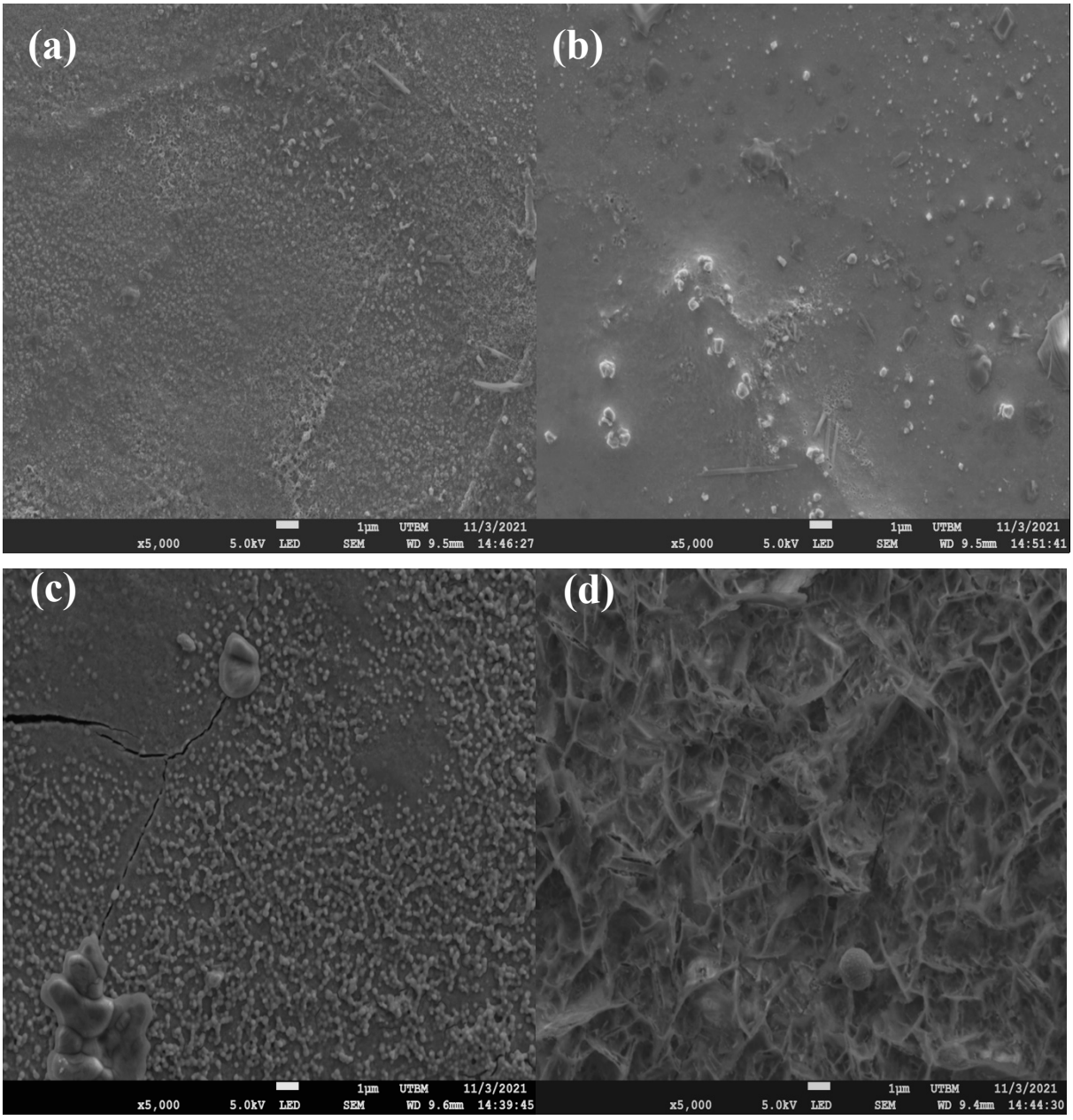

Figure 2. *Secondary electron SEM micrographs of (a) CNTS, (b) CCTS, (c) CMTS and (d) CFTS films deposited by spray pyrolysis at substrate temperature of 280 °C during 30 min.*

Optical characteristics

Figure.3 shows the variations of the absorption coefficient **(α)** as a function of photon energy (hν) for the different thin layers of CNTS, CCTS, CMTS and CFTS. The absorption coefficients of the CNTS and CCTS films at 2.48 eV (or 500 nm corresponding to the maximal irradiance of the solar spectrum) are about 2 10^4 cm^{-1} and then become lower for energy inferior at 1.3 eV (i.e. $\lambda > 950$ nm). Despite a moderate oxidation in the CMTS film, its absorption coefficient remains higher than 10^4 cm^{-1} even in near infrared range [18,19]. Regarding the CFTS film, while its absorption coefficient is slightly lower than 10^4 cm^{-1}, its remains quite stable in the visible range (0.6-1 10^4 cm^{-1} from 1 to 3 eV).

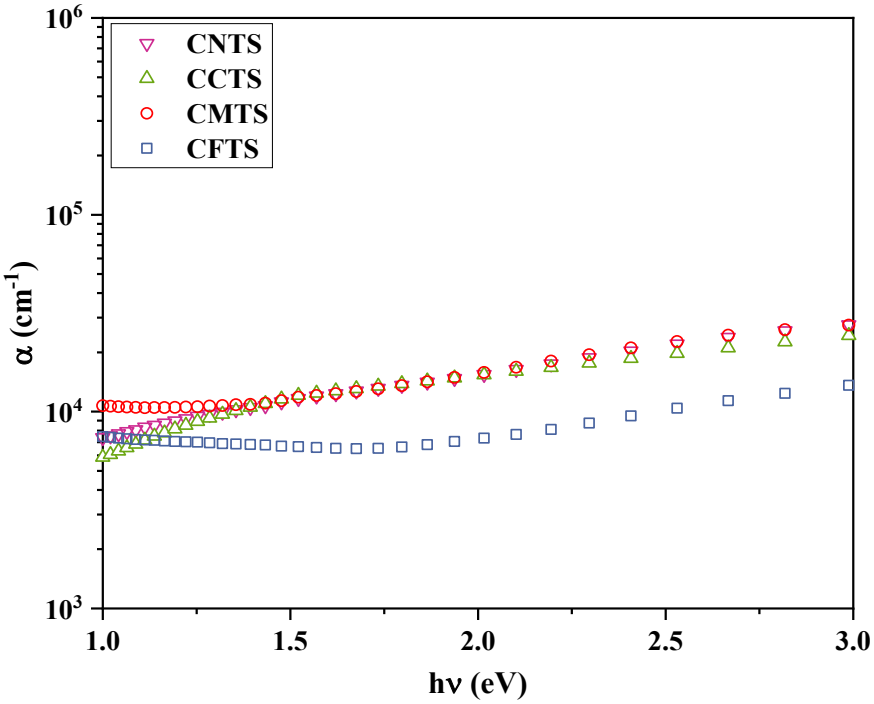

Figure 3. *Evolutions of the absorption coefficient (α) as a function of photon energy (hν) of CXTS thin films deposited at substrate temperature of 280°C during 30min.*

The variation curves of $(\alpha h\nu)^2$ as a function of (hν) for the different thin layers of CXTS, are displayed in Figure.4. Considering a direct transition, and by extrapolating the linear part of the curve $(\alpha h\nu)^2$ on the energy axis, the band gap values Eg of the thin layers of CNTS, CCTS and CMTS are equal to 1.62, 1.58 and 1.64 eV, respectively. These obtained values fall in the top within the desired range (1.10-1.55 eV) found by other authors [20,21,22]. The relatively high values of the optical band gap could be explained by the presence of the secondary phases based on sulfides, or oxide for such CXTS films, which have higher optical band gap value (CuS_2 1.87 eV [23], MnO_2 2.48 eV [24]). On the other hand, the thin layer of CFTS exhibits a value

equal to 2.23 eV. This value is high compared to that of other CXTS film and to that of literature (1.55 eV in [25]). This phenomenon would rather ascribe to the loss of sulfur [15] or more probably to the formation of amorphous oxides, having higher band gap transition (e.g. Fe_2O_3 2.1 eV [26]). The optical properties, such as the absorption coefficient and the value of the optical transition are suitable for a single junction solar cell.

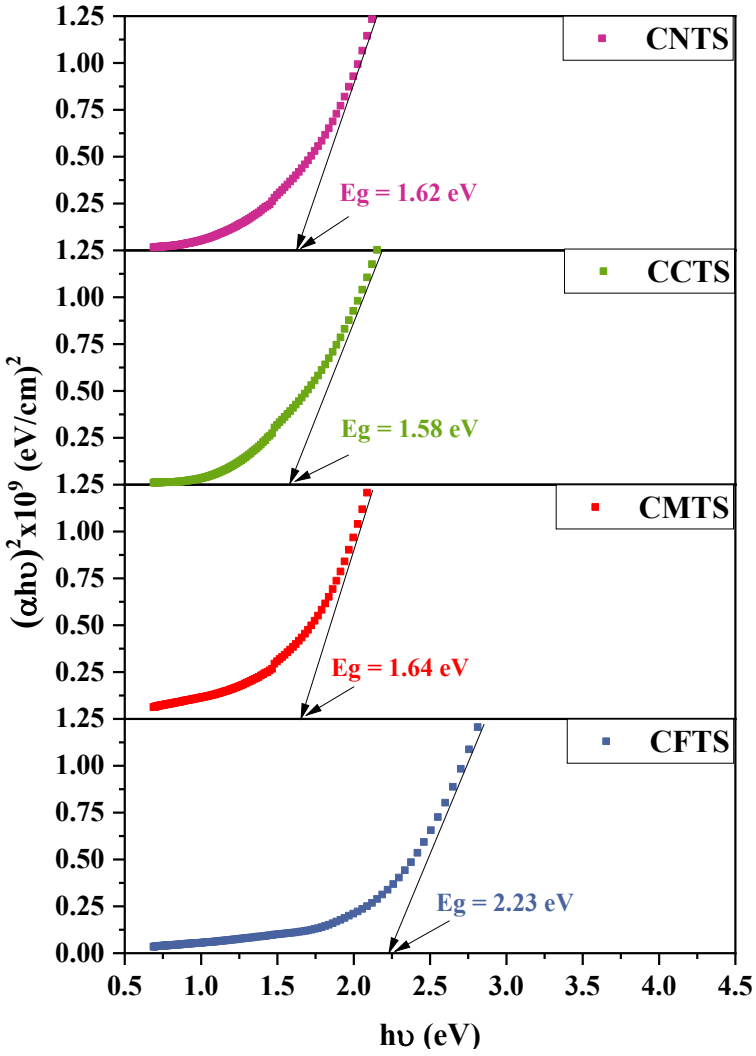

Figure 4. *Variation of $(\alpha h\nu)^2$ as a function of $(h\nu)$ of CXTS thin films deposited at substrate temperature of 280 °C during 30 min.*

- **Electrical properties**

In order to study the electrical properties of thin layers of CXTS prepared by spray pyrolysis in air at 280 °C, the hot-probe method and the four-probe method were used. The results are summarized in Table.3. All the CXTS thin layers present a p-type electrical conductivity

meaning that the holes are the major charge carriers. According to the method, the holes diffusing far from the hot probe will follow the direction of the current in the semiconductor and therefore it is the hot probe, which provides the positive charges to the milliammeter. Moreover, the electrical resistivity for all the layers varies between 2.7 10^{-3} and 2.5 Ω.cm. These values are close to the values (9 10^{-2} Ω.cm) of Al-doped CZTS thin films found by A. S. Gadallah et al. [27]. The lowest value of electrical resistivity is obtained for thin layers of CNTS and CCTS. Several possible reasons can explain this result: the rich content in sulfur as it was reported in the article [27] where the resistivity decreases with the increase in the amount of sulfur, the good crystallinity, the surface homogeneity, the efficient oxidation prevention during the synthesis, the lower stress deposition and the larger crystallite size [14,28]. Furthermore, it is noteworthy that despite the rather strong oxidation observed in CFTS film and the relatively poor crystallization of the stannite CFTS phase, the electrical resistivity value is lower than in CMTS film. The CMTS film exhibits the highest electrical conductivity. The finer grain size compared to other films, and thus the more numerous grain boundaries, would act as charge carrier scatter centers. In addition, the presence of stress as demonstrated by the cracks observation by SEM analyses or calculated by XRD would also affects the electrical transport properties of the stannite CMTS phase [29]. Furthermore, the electrical resistivity of the element, related to the free electrons in the outermost shell, could also contribute to the observed electrical resistivity variation in CXTS film (14 (Mn) < 0.98 (Fe) < 0.70 (Ni) < 0.58 (Co) in 10^{-5} Ω.cm).

Table 4. *Electrical parameters of CXTS thin films deposited at substrate temperature of 280 °C during 30 min.*

Thin films	*Type of conductivity*	*Sheet resistance ($\Omega\, sq^{-1}$)*	*Electrical resistivity (Ω cm)*
CNTS	P	3.8	2.7 10^{-3}
CCTS	P	5.3	3.9 10^{-3}
CMTS	P	2.9 10^{3}	2.5
CFTS	P	3.5 10^{2}	3.1 10^{-1}

Conclusion

In conclusion, thin layers of CNTS, CCTS, CMTS and CFTS were successfully prepared by spray pyrolysis under the same deposition conditions (substrate temperature of 280 °C, air atmosphere, distilled water as solvent agent, deposition time of 30 min). Compositional analyzes by EDS revealed a composition relatively close to the stoichiometry for the layers of CNTS and CCTS and farer from the stoichiometry for CMTS and CFTS due to a sulfur deficiency. A moderate oxidation was also observed in CMTS and in a stronger way in CFTS film. The XRD analyzes showed that the crystallization of the desired phases such as the cubic phase for CNTS and the stannite phase for CCTS, CMTS and CFTS film. The microstructure of the stannite CFTS film is poorly crystallized contrary to the cubic CNTS and tetragonal stannite in CCTS and CMTS combining larger crystallites with lower microstrain values and dislocation densities. The topography of the CNTS, CCTS and CMTS layers exhibit a rather homogeneous and compact surface with nodules distribution, whereas the CFTS surface develops excrescences. The optical analyzes indicated a high absorption coefficient of the order of 10^4 cm^{-1} in the visible range for all the layers and an optical band gap of 1.62, 1.58 and 1.64 eV for the layers CNTS, CCTS and CMTS respectively. A higher band gap was measured in CFTS layers due to the oxidation. The electrical resistivity is about 10^{-3} Ω.cm for CCTS and CNTS layers lower than in CZTS films. In CMTS films, it is believed that the mechanical stress combined with the partial oxidation and the superior electrical resistivity of Mn, are responsible of the higher electrical resistivity. Despite the rather high oxidation of the CFTS, this material exhibits relatively interesting properties, such as the optical absorption or the electrical resistivity. The chemical composition and the microstructure of the cobalt or nickel quaternary sulfides lead to optimized optical and electrical properties suitable as a use for absorbing layer in solar cells. It is demonstrated that the spray pyrolysis technique under air atmosphere with distilled water as solvent agent is a convenient way for the synthesis of sulfide absorbing layer in low cost solar cell industry. Moreover, these materials offer a relatively strong resistance versus the oxidation which could help to ensure the lifetime of such solar cell. However, CFTS and CMTS materials being more sensitive to the oxygen, the deposition in air atmosphere is insufficient to prevent their oxidation even at low deposition temperature resulting in poorer properties and mechanical integrity especially for CMTS film.

Acknowledgements

Part of this work was done within the FEMTO-ST SURFACE platform. The authors would like to acknowledge Pays of Montbéliard Agglomération for their support.

References

[1] S. Ahmadi, N. Khemiri, A. Cantarero, M. Kanzari, XPS analysis and structural characterization of CZTS thin films deposited by one-step thermal evaporation, *J. Alloy. Compd.* **925** (2022) 166520, https://doi.org/10.1016/j.jallcom.2022.166520.

[2] N. M. Shaalan, A. Z. Mahmoud, D. Hamad, Synthesis of CZTS without sulfurization process and its performance evaluation on n-Si substrate as ITO-free photovoltaic cell, *Mater. Sci. Semicond. Process,* **120** (2020) 105318, https://doi.org/10.1016/j.mssp.2020.105318.

[3] S. Dridi, E. Aubry, N. Bitri, F. Chaabouni, and P. Briois, Growth and Characterization of Cu_2MnSnS_4 Thin Films Synthesized by Spray Pyrolysis under Air Atmosphere, Coatings, **963** (2020) 10, https://10.3390/coatings10100963.

[4] J. He, L. Sun, K. Zhang, W. Wang, J. Jiang, Y. Chen, P. Yang, J. Chu, Effect of post-sulfurization on the composition, structure and optical properties of Cu_2ZnSnS_4 thin films deposited by sputtering from a single quaternary target, *Appl. Surf. Sci.* **264** (2013) 133-138, http://dx.doi.org/10.1016/j.apsusc.2012.09.140.

[5] M. Patel, I. Mukhopadhyay, A. Ray, Structural, optical and electrical properties of spray-deposited CZTS thin films under a non-equilibrium growth condition, *J. Phys. D: Appl. Phys.* **45** (2012) 445103, 10.1088/0022-3727/45/44/445103.

[6] P. R. Ghediya, Y. M. Palan, D. P. Bhangadiya, I. I. Nakani, T. K. Chaudhuri, K. Joshi, C. K. Sumesh, J. Ray, Electrical properties of Ag/p-Cu_2NiSnS_4 thin film Schottky diode, *Mater. Today Commun.* **28** (2021) 102697, https://doi.org/10.1016/j.mtcomm.2021.102697.

[7] P. R. Ghediya and T. K. Chaudhuri, Dip-coated Cu_2CoSnS_4 thin films from molecular ink for solar photovoltaics, *Mater. Res. Express,* **5** (8) (2018) 085509, https://doi.org/10.1088/2053-1591/aad475.

[8] A. S. Hassanien, I. M. El Radaf, Optical characterizations of quaternary Cu_2MnSnS_4 thin films: Novel synthesis process of film samples by spray pyrolysis technique, *Physica B: Phys. Condens. Matter*, 585 (2020) 412110, https://doi.org/10.1016/j.physb.2020.412110.

[9] C. Barret, T. B. Massalki, Structure of Metals, Oxford Pergamon, Oxford, (1980), 10.1002/crat.19810160904.

[10] A. Jebali, N. Khemiri, M. Kanzari, The effect of annealing in N_2 atmosphere on the physical properties of $SnSb_4S_7$ thin films, *J. Alloy. Compd.* **673** (2016) 38-46, 10.1016/j.jallcom.2016.02.159.

[11] G. K. Williamson, R. E. Smallman, Dislocation densities in some annealed and cold worked metals from measurements on the X-ray Debye-Scherrer spectrum, *Philos. Mag. 1* (1956) 34-46, https://doi.org/10.1080/14786435608238074.

[12] R. Deepika and P. Meena, Preparation and characterization of quaternary semiconductor Cu_2NiSnS_4 (CNTS) nanoparticles for potential solar absorber materials, *Mater. Res. Express* **6** (2019) 0850b7, https://doi.org/10.1088/2053-1591/ab24e9.

[13] P. S. Maldar, A. A. Mane, S. S. Nikam, S. D. Giri, A. Sarkar, A. V. Moholkar, Temperature dependent properties of spray deposited Cu_2CoSnS_4 (CCTS) thin films, *J. Mater. Sci. - Mater. Electron.* **28** (2017) 18891-18896, 10.1007/s10854-017-7842-1.

[14] A. Ziti, B. Hartiti, A. Belafhaili, H. Labrim, S. Fadili, A. Ridah, M. Tahri, and P. Thevenin, Effect of dip-coating cycle on some physical properties of Cu_2NiSnS_4 thin films for photovoltaic applications, *J. Mater. Sci. - Mater. Electron.* **32** (2021) 16726-16737, https://doi.org/10.1007/s10854-021-06230-9.

[15] P. S. Maldar, M. A. Gaikwad, A. A. Mane, S. S. Nikam, S. P. Desai, S. D. Giri, A. Sarkar, A. V. Moholkar, Fabrication of Cu_2CoSnS_4 thin films by a facile spray pyrolysis for photovoltaic application, *Sol. Energy,* **158** (2017) 89-99, http://dx.doi.org/10.1016/j.solener.2017.09.036.

[16] D. B. Khadka, J. H. Kim, Structural, optical and electrical properties of Cu_2FeSnX_4 (X=S, Se) thin films prepared by chemical spray pyrolysis, *J. Alloy. Compd.* **638** (2015) 103-108, http://dx.doi.org/10.1016/j.jallcom.2015.03.053.

[17] X. Meng, H. Deng, J. Tao, H. Cao, X. Li, L. Sun, P. Yang, J. Chu, Heating rate tuning in structure, morphology and electricity properties of Cu_2FeSnS_4 thin films prepared by sulfurization of metallic precursors, *J. Alloy. Compd.* **680** (2016) 446-451, http://dx.doi.org/10.1016/j.jallcom.2016.04.166.

[18] Z. Seboui, A. Gassoumi, Y. Cuminal, and N. K. Turki, The post-growth effect on the properties of Cu_2ZnSnS_4 thin films, *J. Renew. Sustain. Energy* **7** (2015) 011203, http://dx.doi.org/10.1063/1.4908063.

[19] M. Marzougi, M. Ben Rabeh, M. Kanzari ; Effect of Na doping on structural and optical properties in Cu_2ZnSnS_4 thin films synthesized by thermal evaporation Method, *Thin Solid Films,* 672 (2019) 41-46, https://doi.org/10.1016/j.tsf.2018.12.046.

[20] P.S. Maldar, A.A. Mane, S.S. Nikam, S.D. Dhas, A.V. Moholkar, Spray deposited Cu_2CoSnS_4 thin films for photovoltaic application: Effect of film thickness, *Thin Solid Films* **709** (2020) 138236, https://doi.org/10.1016/j.tsf.2020.138236.

[21] K. Mokurala, S. Mallick, P. Bhargava, S. Siol, T. R. Klein, M. F.A.M. van Hest, Influence of dipping cycles on physical, optical, and electrical properties of Cu_2NiSnS_4: Direct solution dip coating for photovoltaic applications, *J. Alloy. Compd.* **725** (2017) 510-518, 10.1016/j.jallcom.2017.07.188.

[22] L. Chen, H. Deng, J. Tao, W. Zhou, L. Sun, F. Yue, P. Yang, J. Chu, Influence of annealing temperature on structural and optical properties of Cu_2MnSnS_4 thin films fabricated by sol-gel technique, *J. Alloy. Compd.* **640** (2015) 23-28, http://dx.doi.org/10.1016/j.jallcom.2015.03.225.

[23] N. Bouguila, Y. Bchiri, M. Kraini, R. Souissi, N. Hafienne, C. Vázquez-Vázquez, S. Alaya , Investigation of some physical and photoconductive properties of sprayed CuS_2 film, *J. Mater. Sci. - Mater. Electron.* **33** (2022) 3810-3821, https://doi.org/10.1007/s10854-021-07572-0.

[24] S. Manikandan, D. Sasikumar, Improving sunlight-photocatalytic activity of undoped and phosphorus doped MnO_2 with activated carbon from bio-waste with nanorods morphology, *Inorg. Chem. Commun.* **144** (2022) 109942, https://doi.org/10.1016/j.inoche.2022.109942.

[25] S. Dridi, G. El Fidha, N. Bitri, F. Chaabouni and I. Ly, Synthesis of chemical spray pyrolyzed Cu_2FeSnS_4 thin films for solar cells, *Indian J. Phys.* **94** (2019) 6, https://doi.org/10.1007/s12648-019-01539-y.

[26] E. Aubry, T. Liu, A. Dekens, F. Perry, S. Mangin, T. Hauet, A. Billard, Synthesis of iron oxide films by reactive magnetron sputtering assisted by plasma emission monitoring, *Mater. Chem. Phys.* **223** (2019) 360-365, https://doi.org/10.1016/j.matchemphys.2018.11.010.

[27] A. S. Gadallah, M. A. Salim, T. Atwee, A. M. Ghander, Effect of Al doping on structural, morphological, optical, and electrical properties of Cu_2ZnSnS_4 thin films prepared by sol-gel spin coating, Optik **159** (2018) 275-282, https://doi.org/10.1016/j.ijleo.2018.01.086.

[28] A. Chihi, M. F. Boujmil and B. Bessais, Synthesis and characterization of photoactive material Cu_2NiSnS_4 thin films, *J. Mater. Sci. - Mater. Electron.* **30** (2019) 3338-3348, https://doi.org/10.1007/s10854-018-00607-z.

[29] J. R. Bautista, F. Avilés, A.I. Oliva, O. Ceh, J.E. Corona, Correlations between mechanical stress, electrical conductivity and nanostructure in Al films on a polymer substrate, *Mater. Charact.* **61** (2010) 325 – 329, https://doi.org/10.1016/j.matchar.2009.12.016.